Dalton Transactions

Cite this: *Dalton Trans.*, 2012, **41**, 2084

www.rsc.org/dalton

PAPER

Water oxidation catalyzed by a new tetracobalt-substituted polyoxometalate complex: $[\{Co_4(\mu\text{-}OH)(H_2O)_3\}(Si_2W_{19}O_{70})]^{11-}$†

Guibo Zhu,[a] Yurii V. Geletii,[a] Paul Kögerler,[b] Helmut Schilder,[b] Jie Song,[a] Sheri Lense,[a] Chongchao Zhao,[a] Kenneth I. Hardcastle,[a] Djamaladdin G. Musaev[c] and Craig L. Hill*[a]

Received 27th June 2011, Accepted 17th October 2011
DOI: 10.1039/c1dt11211b

A new polyoxometalate of earth adundant elements $[\{Co_4(\mu\text{-}OH)(H_2O)_3\}(Si_2W_{19}O_{70})]^{11-}$ has been synthesized, characterized and shown to be a water oxidation catalyst. The initial catalytic complex is unstable and slowly undergoes hydrolysis. The hydrolysis products have been isolated and characterized, and their catalytic water oxidation activity is assessed.

Introduction

Development of a stable and efficient water oxidation catalyst (WOC) is a central challenge in thermal and photochemical energy technologies requiring the use of water as a source of electrons.[1,2] As a result, many new homogeneous[3–19] and heterogeneous[20–30] WOCs have been reported recently. Various defect polyoxometalates (POMs) are attractive as ligands for WOCs because they can strongly bind multiple transition metal centers proximal to one another, a helpful attribute for facilitating multi-electron processes, including the 4-electron oxidation of H_2O to O_2. At the same time, POMs are oxidatively, hydrolytically (over various pH ranges) and thermally stable.[31–38] Recently and simultaneously our group[39–42] and that of Bonchio[43–46] reported the synthesis of $[Ru^{IV}_4O_4(OH)_2(OH_2)_4(\gamma\text{-}SiW_{10}O_{36})_2]^{12-}$ (**Ru4**) by different methods and demonstrated the ability of this POM to catalyze water oxidation by $[Ru(bpy)_3]^{3+}$ buffered at pH 7 (our group[39–42]) or by Ce(IV) at very acidic pH values (Sartorel *et al.*[43–46]). Subsequently multiple oxidation states of **Ru4** were thoroughly characterized and the $Ru(V)_4$ oxidation state of **Ru4** was identified as the one that releases O_2.[42] Later, the analogous phosphorous-centered POM, $Cs_{10}[(\gamma\text{-}PW_{10}O_{36})_2Ru^{IV}_4O_6(OH_2)_4]\cdot 17H_2O$ was synthesized and also shown to be a water oxidation catalyst.[47] Most recently, we reported that the carbon-free complex $[Co_4(H_2O)_2(PW_9O_{34})_2]^{10-}$ (**1**), based on earth abundant elements (Co, W, and P), is a stable and efficient water oxidation catalyst.[48] We reasoned that a Si-centered analogue of **1**, might be an even more active WOC. However, we repeatedly failed to isolate this complex using a procedure described by Zhang *et al.*[49] Instead, we obtained an unknown complex, $[\{Co_4(\mu\text{-}OH)(H_2O)_3\}(Si_2W_{19}O_{70})]^{11-}$ (**2**). Here, we report the structural, magnetic, catalytic water oxidation activity, and hydrolytic properties of **2**.

[a]*Department of Chemistry, Emory University, Atlanta, GA, 30322, USA*
[b]*Institut für Anorganische Chemie, RWTH Aachen University, D-52074, Aachen, Germany*
[c]*Cherry L. Emerson Center for Scientific Computation, Emory University, Atlanta, GA, 30322. E-mail: chill@emory.edu; Fax: (+1)404-727-6076; Tel: (+1)404-727-6611*

† Electronic supplementary information (ESI) available: X-ray structure of $\mathbf{K_{10}Na\text{-}3}$, IR spectra of $\mathbf{K_{10.2}Na_{0.8}}$-**2** and $\mathbf{K_{10}Na\text{-}3}$, TGA of $\mathbf{K_{10.2}Na_{0.8}}$-**2** and $\mathbf{K_{10}Na\text{-}3}$, and cyclic voltammetric behavior of $\mathbf{K_{10.2}Na_{0.8}}$-**2** in buffer solution. CCDC reference numbers 832126 and 832127. For ESI and crystallographic data in CIF or other electronic format see DOI: 10.1039/c1dt11211b

Experimental

Materials and methods

$Na_{10}[\alpha\text{-}SiW_9O_{34}]\cdot 18H_2O$ was prepared by the literature procedure. The purity was checked by IR spectroscopy.[50] All reagents used were commercially available and were used as received. Elemental analyses for K, Na, Co, Si and W were performed by Galbraith Laboratories (Knoxville, Tennessee). IR spectra (2% sample in KBr pellet) were recorded on a NicoletTM 6700 FT-IR spectrometer. The electronic absorption spectra were taken on an Agilent 8453 UV-vis spectrometer. The thermogravimetric data were collected on an ISI TGA 1000 instrument. Electrochemical data were obtained at room temperature using a BAS CV-50W electrochemical analyzer equipped with a glassy-carbon working electrode, a Pt-wire auxiliary electrode, and a Ag/AgCl (3 M NaCl) BAS reference electrode. All oxidation potentials are reported relative to this reference electrode. Temperature-dependent magnetic susceptibility measurements of potassium, sodium salt of **2**, $\mathbf{K_{10.2}Na_{0.8}}$-**2** were performed on polycrystalline samples using a Quantum Design MPMS-XL5 SQUID magnetometer (2–290 K, 0.1 Tesla) and cylindrical PTFE sample holders. Susceptibility data were corrected for diamagnetic contributions (χ_{dia}($\mathbf{K_{10.2}Na_{0.8}}$-**2**) = -747.2×10^{-6} cm^3 mol^{-1}). Comprehensive descriptions of computational details in the magnetochemical analysis of the Co(II)-based systems have been published.[51,52]

Synthesis

$\mathbf{K_{10.2}Na_{0.8}}$[$\{Co_4(\mu\text{-}OH)(H_2O)_3\}(Si_2W_{19}O_{70})$]·31$H_2O$ ($\mathbf{K_{10.2}Na_{0.8}}$-2). $Na_{10}[\alpha\text{-}SiW_9O_{34}]\cdot 18H_2O$ (0.8 g, 0.3 mmol) was dissolved in

15 mL of water. The pH was adjusted to 6.8 by 1 M HCl, then, 190 mg (0.8 mmol) of $CoCl_2 \cdot 6H_2O$ were added. The pH dropped to ~5. This solution was heated to 80 °C for 1 h. Some precipitation became visible. After cooling the solution to room temperature, the pH was ~6.5. Subsequently the pH was adjusted to 5.8 by 0.5 M HCl. Addition of 2 mL of saturated aqueous KCl solution to the suspension and stirring for 10 min produced a precipitate which was filtered. Red block crystals were collected from the reaction solution after 24 h. Yield: 18% based on W. IR (KBr, ν/cm^{-1}): 992 (m), 946 (m), 888 (s), 786 (s), 703 (s), 668 (sh), 600 (m), 536 (sh), 523(m). Elemental analysis calculated (found) for $K_{10.2}Na_{0.8}[\{Co_4(\mu\text{-}OH)(H_2O)_3\}(Si_2W_{19}O_{70})] \cdot 31H_2O$: K: 6.70 (6.60); Na: 0.309 (0.296); Co: 3.96 (3.76); Si: 0.944 (0.938); W: 58.7 (58.4) %.

$K_{10}Na[\{Co(H_2O)\}(\mu\text{-}H_2O)_2K\{Co(H_2O)_4\}(Si_2W_{18}O_{66})] \cdot 25\ H_2O$ (K_{10}Na-3). **$K_{10.2}Na_{0.8}$-2** (150 mg) was dissolved in 4 mL of water. Then, 1 mL of 1 M KOAc/HOAc buffer (pH 4.8) and 2 mL of 1 M NaOAc/HOAc buffer (pH 4.8) were added. Slow evaporation at room temperature results in crystals after one week. The geometrical structure of the polyanion in **K_{10}Na-3** is virtually identical to that of 1Co2-K(A) in ref. 54. The structure of the polyanion is depicted in Figure S1.† IR (KBr, ν/cm^{-1}): 997 (m), 942 (m), 884 (s), 863 (m), 803 (m), 730 (s), 651 (m), 547 (w), 525 (w). Elemental analysis calculated (found): K: 7.55 (7.56); Na: 0.404 (0.653); Co: 2.07 (2.19); Si: 0.986 (0.901); W: 58.1 (57.6) %.

X-Ray crystallography

Single crystals suitable for X-ray structure analysis were each coated with Paratone-N oil, suspended on a small fiber loop and placed in a cooled nitrogen gas stream at 173 K on a Bruker D8 APEX II CCD sealed tube diffractometer with graphite monochromator Mo-Kα (λ = 0.71073 Å) radiation. Data were measured using a combination of φ and ω scans with 10 s frame exposure and 0.3° frame widths. Data collection, indexing and initial cell refinements were all carried out using SMART.[53] Frame integration and final cell refinements were done using SAINT.[54] The molecular structure of each complex was determined using direct methods and Fourier techniques, and refined by the standard full-matrix least-squares procedure. A multiple absorption correction, including face indexing, was applied using the program SADABS.[55] The largest residual electron density for each structure was located close to (less than 1.0 Å from) the W atoms and was most likely due to imperfect absorption corrections frequently encountered in heavy-metal atom structures. Scattering factors and anomalous dispersion corrections are taken from the International Tables for X-ray Crystallography. Structure solution, refinement, graphic and generation of publication materials were performed by using SHELXTL, v 6.14 software.[56] The crystal data and structure refinement parameters are summarized in Table 1.

Catalytic experiments

Water oxidation was performed in a 10 mL Schlenk flask. The vessel was filled with 8 mL of a solution containing 1.0 mM $[Ru(bpy)_3]Cl_2$, 5 mM $Na_2S_2O_8$, 25 mM buffer solution and the desired concentration of catalyst. The solution was carefully deairated by bubbling argon. The reaction was initiated by exposing the reaction vessel to the light (Xe lamp filtered with a 420–520 nm band-pass filter). After the desired illumination time, the reaction was temporarily stopped by blocking the light, and the

Table 1 Crystal data and structural refinement for the X-ray structure analyses of **$K_{10.2}Na_{0.8}$-2** and **K_{10}Na-3**

	$K_{10.2}Na_{0.8}$-2	**K_{10}Na-3**
Molecular formula	$Co_4\ H_{69}K_{10.2}\ Na_{0.8}\ O_{105}\ Si_2\ W_{19}$	$Co_2\ H_{64}K_{10}\ Na\ O_{98}\ Si_2\ W_{18}$
Formula wt./g mol^{-1}	5951.54	5529.58
T/K	173(2)	173(2)
Radiation (λ)/Å	0.71073	0.71073
Crystal system	Triclinic	Triclinic
Space group	$P\bar{1}$	$P\bar{1}$
a/Å	13.049(7)	14.632(4)
b/Å	17.315 (9)	18.179 (4)
c/Å	22.642(12)	18.284(4)
α (°)	67.540(8)	65.974(3)
β (°)	74.221(8)	79.207(4)
γ (°)	84.294 (8)	86.471 (4)
V/Å^3	4550(4)	4362.8(18)
Z	2	2
ρ_c/g cm^{-3}	4.111	3.987
μ/mm^{-1}	25.223	24.607
F(000)	4918	4570
Crystal size/mm	0.44 × 0.35 × 0.31	0.29 × 0.19 × 0.16
Reflections collected	73185	74967
Independent reflections	20048	20765
Absorption correction	Multi-scan	Integration
Refinement method	Full-matrix least-squares on F^2	Full-matrix least-squares on F^2
Goodness-of-fit on $\lvert F \rvert^2$	1.053	1.026
Final R indices		
$[R > 2\sigma(I)]$	$R_1{}^a = 0.0554$, $wR_2{}^b = 0.1910$	$R_1{}^a = 0.0449$, $wR_2{}^b = 0.1125$
R indices (all data)	$R_1{}^a = 0.0667$, $wR_2{}^b = 0.2050$	$R_1{}^a = 0.0581$, $wR_2{}^b = 0.1204$
Largest diff. peak and hole/e Å^{-3}	3.555 and –8.785	7.293 and –6.896

^{a} $R_1 = \Sigma \lVert F_0 \rvert - \lvert F_c \rVert / \Sigma \lvert F_0 \rvert$; ^{b} $wR_2 = \Sigma[w(F_0^2 - F_c^2)^2] / \Sigma[w(F_0^2)^2]^{1/2}$.

flask was vigorously shaken to allow equilibration of O_2 between the solution and the head-space. Analysis of the headspace gas was performed by withdrawing a 0.1 mL sample from the headspace and using a gas chromatograph Agilent 7890A equipped with thermal conductivity detector and a GC capillary column with 5 Å molecular sieves to separate O_2 and N_2. Argon was used as the carrier gas. The reaction was complete after consumption of $Na_2S_2O_8$. The amount of N_2 detected allowed the correction for the air leaking in the reaction vessel. The detection limit for O_2 was 0.02 μmol.

Results and discussion

Description of crystal structures

$K_{10.2}Na_{0.8}[\{Co_4(\mu\text{-}OH)(H_2O)_3\}(Si_2W_{19}O_{70})]\cdot 31H_2O$ ($K_{10.2}Na_{0.8}$-2). The symmetry of the complex is C_1 and the Co1 and W8 moieties are disordered, resulting in two possible polyanion structures (2a and 2b) shown in Fig. 1. The best refinement was obtained with occupation factors of 1/2 for each polyanion. Bond valence sum calculations reveal that the three terminal oxygens associated with the Co_4 cluster are all diprotonated; the only μ-oxo oxygen is monoprotonated. The connection motif of the cobalt atoms (Fig. 1c and 1d) is rarely seen in polyanion chemistry. This polyanion exhibits an asymmetric dimeric structure, composed of $[A\text{-}\alpha\text{-}SiW_9O_{34}]^{10-}$ and $[\alpha\text{-}SiW_{10}O_{37}]^{10-}$ units, which are linked by a Co_4 cluster. The central Co_4 cluster contains three octahedrally coordinated Co^{2+} ions and one tetragonal pyramidally coordinated Co^{2+} ion. The $Co2O_6$ and $Co4O_6$ units (octahedral Co centres) and the $Co3O_5$ unit (a tetragonal pyramid which is weakly bonded to $O_{27}W$) located at the trivacant sites of $[A\text{-}\alpha\text{-}SiW_9O_{34}]^{10-}$ are used to complete the α-Keggin structure $[\alpha\text{-}SiCo_3W_9O_{40}]^{16-}$. At the same time, $Co2O_6$ and $Co1O_6$ units (or $Co1AO_6$) replace two corner-sharing WO_6 octahedra from $[\alpha\text{-}SiW_{12}O_{40}]^{4-}$, resulting in the well-defined α-Keggin structure $[\alpha\text{-}SiCo_2W_{10}O_{40}]^{12-}$. The crucial factor in the synthesis of **$K_{10.2}Na_{0.8}$-2** is the use of high concentrations of potassium ions for crystallization. If insufficient potassium chloride is added, no red crystals can be obtained.

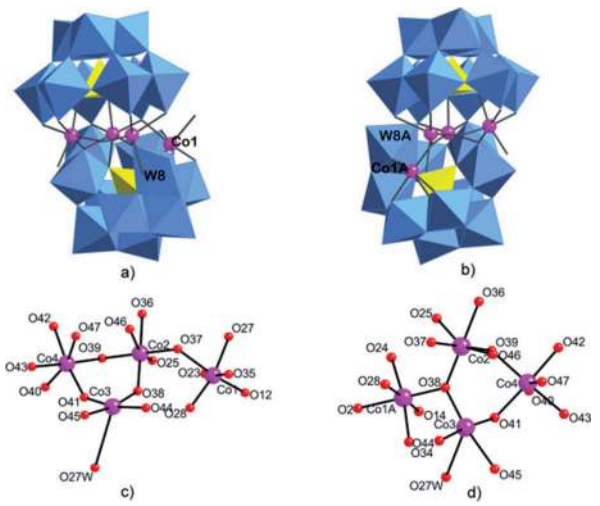

Fig. 1 The two isomers of $[\{Co_4(\mu\text{-}OH)(H_2O)_3\}(Si_2W_{19}O_{70})]^{11-}$ (**2a** and **2b**) coexisting in a 1 : 1 ratio in the single-crystal structure of **$K_{10.2}Na_{0.8}$-2**. The cobalt centers (purple) are shown in ball-and-stick notation, the polyoxometalate framework in polyhedral notation (WO_6 octahedra: blue, SiO_4 tetrahedra: yellow). Hydrogen atoms are omitted for clarity. Lower panels (c) and (d) show the μ-oxo connection motifs of the cobalt sites in **2a** and **2b**, respectively.

Magnetic properties of $[\{Co^{II}_4(\mu\text{-}OH)(H_2O)_3\}(Si_2W_{19}O_{70})]^{11-}$, 2. In order to probe whether an equal mixture of the two possible structural scenarios involving the W8/Co1 distribution (Fig. 1), **2a** and **2b**, are commensurate with observable magnetic characteristics, low-field susceptibility measurements (2–290 K, 0.1 and 1.0 Tesla) were performed and analyzed. Our computational framework CONDON, recently expanded to model polynuclear Co(II) clusters,[57] was used to simulate the two scenarios of a Co(II) spin tetrahedron with one (**2b**, Fig. 1d) or two (**2a**, Fig. 1c) missing edges between the basal $\{Co_3\}$ triangle and the apex, defined as either Co4 (**2a**) or Co1 (**2b**). In both cases, we assume uniform exchange coupling J_1 within the triangular $\{Co_3\}$ base, primarily mediated by three μ_2-O bridges (**2a**) or by a single μ_3-O center (**2b**). The exchange energy J_2 between the triangle and the outer ("apical") Co site is also due to μ-*O*-mediated coupling (**2a**: O37; **2b**: O39,O41).

Generally, significant orbital contributions and the resulting strong magnetic anisotropy complicate the analysis of Co(II) species with octahedral ligand fields ($^4T_1$), and the canonical models are only applicable within narrow temperature limits. Thus, modeling the two scenarios **2a** and **2b** was based on a spin Hamiltonian accounting for not only exchange interactions and Zeeman splitting, but also spin–orbit coupling and ligand field effects. Ligand fields are approximated as cubic and uniform for all four Co environments (to avoid overparametrization). Within the constraints of this model, least-squares fitting to the 0.1 and 1.0 Tesla experimental data (Fig. 2) yields the following parameter sets (SQ = 2.7%): For **2a**, ferromagnetic intra-triangle coupling J_1 = +0.5 cm^{-1}, and J_2 = –1.91 cm^{-1}; for **2b**, J_1 = +2.0 cm^{-1}, and J_2 = –1.64 cm^{-1}. These anti- and the ferromagnetic exchange energies are in line with the Co–O–Co angles of the respective exchange pathways. The ligand field parameters (in Wyborne notation) B^4_0 amount to 30900 cm^{-1} (**2a**) and 24350 cm^{-1} (**2b**), common values for slightly distorted CoO_6 environments. The fitting procedure employed fixed, standard values for the Racah parameter B = 825 cm^{-1} and a spin–orbit coupling constant ζ = 533 cm^{-1} for all Co(II) sites.

Catalytic properties

To probe the catalytic activity of **2** towards water oxidation at pH 5–9, we used $[Ru(bpy)_3]^{3+}$, generated *in situ*, as an oxidant.[39,41,42,47,48,58] It can be prepared either as solid material and then used as a stoichiometric oxidant, or photogenerated from $[Ru(bpy)_3]^{2+}$ (λ_{max} = 454 nm, $\varepsilon = 1.4 \times 10^4$ M^{-1} cm^{-1}) in the presence of $S_2O_8^{2-}$ as a sacrificial electron acceptor, eqn (1).[41,47,58]

$$2\,[Ru(bpy)_3]^{2+} + S_2O_8^{2-} + h\nu \rightarrow 2\,[Ru(bpy)_3]^{3+} + 2\,SO_4^{2-} \quad (1)$$

This light-driven process is well studied,[41] and proceeds *via* quenching of the excited state $[Ru(bpy)_3]^{2+*}$ by $S_2O_8^{2-}$, producing $[Ru(bpy)_3]^{3+}$ and $SO_4^{\bullet-}$.[59,60] The $SO_4^{\bullet-}$ produces a second molecule of $[Ru(bpy)_3]^{3+}$. Four equivalents of $[Ru(bpy)_3]^{3+}$ are required to

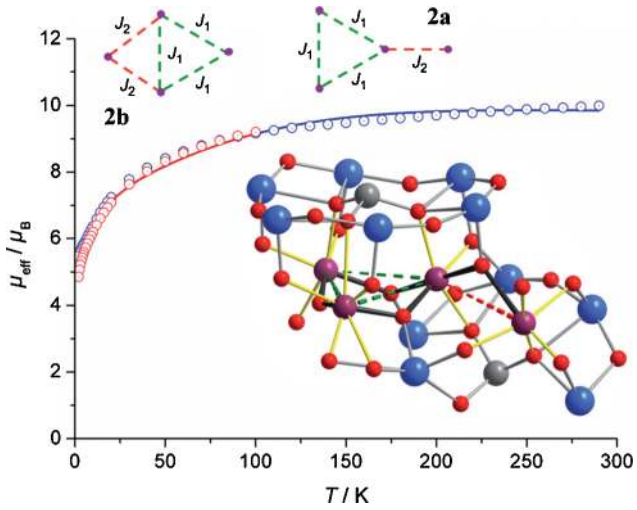

Fig. 2 Temperature dependence of μ_{eff} of **$K_{10.2}Na_{0.8}$-2** (circles: experimental data, graphs: best fits to Hamiltonian based on an equal ratio of scenarios **2a** and **2b**, with exchange patterns defined as in top panel) at 0.1 (blue) and 1.0 (red, < 100 K) Tesla. Inset: Binding modes of the Co_4O_4 fragment in **2a** betwixt adjacent tungstate and silicate groups. The Co–O bonds forming the dominating magnetic exchange pathways are highlighted in dark grey; remaining Co–O bonds completing the Co coordination environments are shown in yellow. Exchange contacts: dashed green (J_1)/ red (J_2) lines. W: blue, Si: grey, O: red, Co: purple spheres.

oxidize two water molecules generating O_2 and four protons (eqn (2)):‡

$$2\,S_2O_8^{2-} + 2\,H_2O + 2\,h\nu \rightarrow 4\,SO_4^{2-} + O_2 + 4\,H^+ \qquad (2)$$

The exemplary kinetics of O_2 formation in eqn (2) (expressed in turnover numbers, TON = $n(O_2)/n(\text{cat})$) and the experimental conditions are given in Fig. 3.

The O_2 yield increases with pH and the TON approaches ~80 (Fig. 3). At present, the rate-limiting step of overall reaction in eqn (2) is not established. Therefore only the initial apparent turnover frequency, defined as TOF_{ap} = TON/time, is estimated, and this value is ~0.1 s^{-1}. The O_2 yield based on $S_2O_8^{2-}$, eqn (2), is around 24%. The reaction conditions were not optimized, and only catalyst concentrations were varied. A decrease of catalyst concentration results in a decrease of both TON and TOF_{ap}.

Stability of 2

The stability of the catalyst under turnover conditions was a key point of interest. First, we evaluated the hydrolytic stability of **2**. In water, this complex has a very low absorbance in the range 450–700 nm. Therefore we measured the spectral changes of **2** at relatively high concentrations (4–6 mM) *versus* time at different pH values. In plain water (natural pH ~ 8) we observed a noticeable absorbance increase (*ca.* 7% after 12 h) in the range 470–550 nm, prompting examination of the stability of **2** in 25 mM sodium acetate (pH 4.8), phosphate (pH 7.2) and borate (pH 9.0) buffer solutions. The initial changes in UV-Vis spectra in borate buffer at pH 9.0 are shown in Fig. 4. A similar pattern was observed

‡ At present we cannot rule out that in our system water is oxidized through 2-electron mechanisms with H_2O_2 formation as an unstable intermediate en route to O_2.

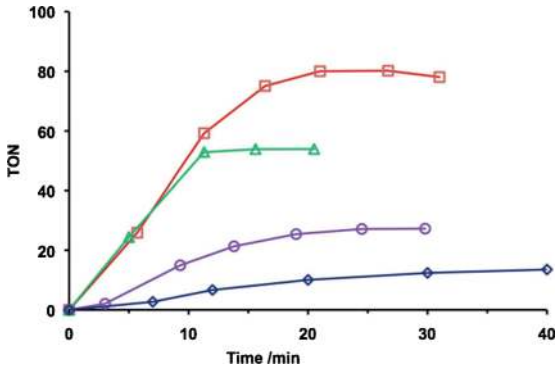

Fig. 3 Kinetics of catalytic light-induced O_2 formation from water by persulphate oxidation in different buffer solutions. Conditions: Xe lamp, 420–520 nm band-pass filter, 1.0 mM $[Ru(bpy)_3]Cl_2$, 5 mM $Na_2S_2O_8$, 25 mM buffer, 10.0 μM **2**, total solution volume 8 mL. Blue diamonds: sodium phosphate buffer, pH 7.2; open purple circles: 1 : 1 mixture of sodium phosphate and sodium borate buffers, pH 8; green triangles: sodium borate buffer, pH 8; red squares: sodium borate buffer, pH 9.§

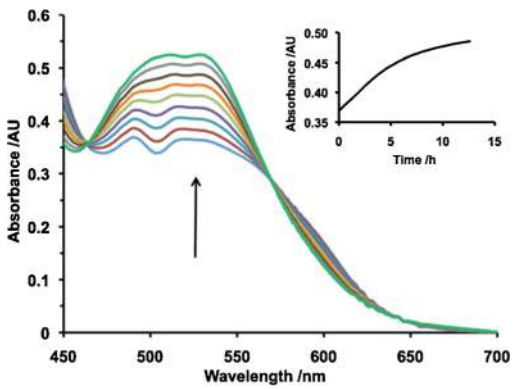

Fig. 4 Changes in UV-Vis spectra of 6.2 mM **2** in 25 mM sodium borate buffer at pH 9.0. The insert is an increase of absorbance at 489 nm with time.

in sodium acetate and phosphate buffered solutions. At pH 9.0 the increase in absorbance was *ca.* 3 times faster than at pH 4.8. Longer aging leads to a notably different final spectrum (Fig. 5). It takes about 40 days to complete the spectral evolution in water. We attempted to crystallize the product compound directly from the aged solutions by slow evaporation of water, but rather than crystals only a pink powder was obtained. Therefore, we aged **2** in acetate buffer solution (pH 4.8) for about one week, and X-ray quality crystals of the resulting **K_{10}Na-3** were obtained by slow evaporation of water. After collection of the complex **K_{10}Na-3**, the solution was left to evaporate more water, and dark red crystals of a salt of $[Co(H_2O)SiW_{11}O_{39}]^{6-}$ (**4**)[61] were obtained (the counter cation(s) were not identified).

Based on literature studies,[62,63] the $[\alpha\text{-}Si_2W_{18}O_{66}]^{16-}$ framework in **3** is an intermediate between the monomer $[A\text{-}\alpha\text{-}SiW_9O_{34}]^{10-}$ and the hypothetical $[\alpha\text{-}Si_2W_{18}O_{62}]^{8-}$ Wells–Dawson anion. The K^+ ion in the central pocket plays a key role in the stabilizing **3** in solution. It bridges the two half-anions and provides rigidity to the metal-oxide framework. In **2**, a $\{Co_4\}$ unit links $[A\text{-}\alpha\text{-}SiW_9O_{34}]^{10-}$

§ A short "induction" period in the kinetic curves is often observed and is caused by a slow mass-transfer of O_2 into a head-space.

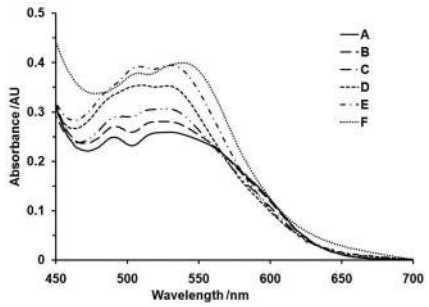

Fig. 5 Time profile of the electronic absorption spectra of **2** (5.7 mM) in water after 0 h (A), 4.5 h (B), 22 h (C), 4 days (D), 10 days (E) and 40 days (F). Conditions: l = 1 cm, 25 °C.

and [α-$SiW_{10}O_{37}$]$^{10-}$, therefore the tungstosilicate framework in **2** could be an unstable intermediate on the way to production of the monomer [A-α-SiW_9O_{34}]$^{10-}$ and an open Wells-Dawson unit, [α-$Si_2W_{18}O_{66}$]$^{16-}$. Complex **3** is a quite kinetically stable compound, but it further converts to the thermodynamically more stable mono-substituted Keggin derivative, **4**, after aging for 1 month (Fig. 6). UV-vis spectra also indicate this stable compound is **4** (Fig. 7).

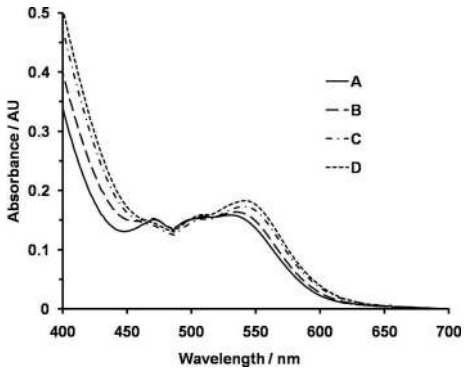

Fig. 6 Time profile of the electronic absorption spectra of **3** (4.7 mM) in water after 0 day (A), 5 days (B), 23 days (C) and 30 days (D). Conditions: l = 1 cm, 25 °C.

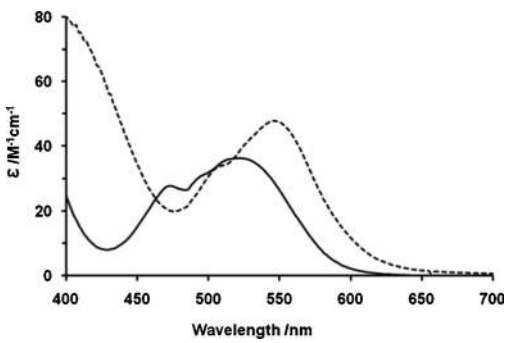

Fig. 7 UV-vis spectra of **K_{10}Na-3** (solid line) and **4** (dashed line).

We attempted to simulate the UV-vis spectrum of aged solution of **2** (after 40 days) by combining UV-vis spectra of **K_{10}Na-3**, **4**, and Co_{aq}^{2+} (as $CoCl_2$). A reasonably good simulation was achieved by combining the spectra of **4** and Co_{aq}^{2+} with 1 : 5.5 ratio (Fig. 8). The remaining difference might be assigned to the

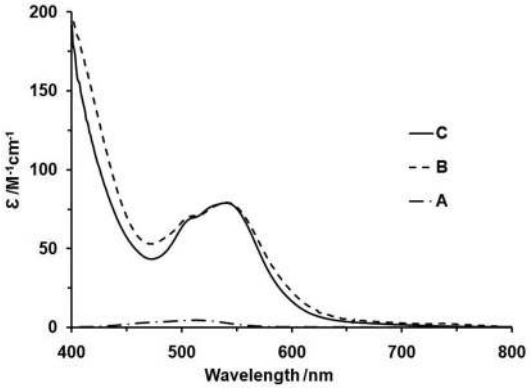

Fig. 8 Simulation of the spectrum of aged solution of **2**: $[Co(H_2O)_6]^{2+}$ (as $CoCl_2$) (A), aged solution of **2** after 40 days (B) and simulation (C).

presence of small amounts of **K_{10}Na-3** and other unidentified compounds. Thus **K_{10}Na-3** is thermodynamically unstable and is consequently absent in the 40-day aged solution. As a consequence, at least three compounds form during aging of aqueous solutions of **2**.

As a result, the most likely decomposition of **2** can be roughly described by the following equations (pK_a of $[Co(H_2O)]^{2+}$ is around 10):[64,65]

$$[\{Co_4(\mu\text{-}OH)(H_2O)_3\}(Si_2W_{19}O_{70})]^{11-} + K^+ + 9\,H_2O + H^+ \rightarrow [\{Co(H_2O)\}(\mu\text{-}H_2O)_2K\{Co(H_2O)_4\}(Si_2W_{18}O_{66})]^{11-} + 2\,[Co(H_2O)_6]^{2+} + WO_4^{2-} \quad (3)$$

$$[\{Co(H_2O)\}(\mu\text{-}H_2O)_2K\{Co(H_2O)_4\}(Si_2W_{18}O_{66})]^{11-} + 4\,WO_4^{2-} + 8\,H^+ \rightarrow 2\,[Co(H_2O)SiW_{11}O_{39}]^{6-} + K^+ + 10\,H_2O \quad (4)$$

The overall reaction is eqn (5):

$$4\,[\{Co_4(\mu\text{-}OH)(H_2O)_3\}(Si_2W_{19}O_{70})]^{11-} + 3\,K^+ + 12\,H^+ + 50H_2O \rightarrow 3[\{Co(H_2O)\}(\mu\text{-}H_2O)_2K\{Co(H_2O)_4\}(Si_2W_{18}O_{66})]^{11-} + 2\,[Co(H_2O)SiW_{11}O_{39}]^{6-} + 8\,[Co(H_2O)_6]^{2+} \quad (5)$$

Catalytic activity of aged solution of 2

Since **2** decomposes slowly in aqueous solution, the question arises: is it the actual water oxidation catalyst? In our previous paper[48] we used 2,2′-bipyridine (bpy) as a poisoning agent to selectively inhibit the activity of $[Co(H_2O)_6]^{2+}$. Addition of bpy to $[Co(H_2O)_6]^{2+}$ results in rapid formation of $[Co(bpy)_3]^{2+}$ which is catalytically inactive for water oxidation. However, addition of three equivalents of bpy per cobalt to a freshly prepared solution of **2** in water results in immediate precipitation. Slow evaporation of the filtrate in a vessel open to air results in formation of crystals. Preliminary X-ray studies show that these crystals contain $[Co(H_2O)SiW_{11}O_{39}]^{6-}$ with $[Co(bpy)_3]^{2+}$ as counterion(s). In contrast to complex **1**, bpy quickly removes Co centers from **2**, consistent with **2** being significantly less stable than **1**.

We meticulously studied the activity of aged stock solutions of **2** prepared in plain water, comparing with the activity of freshly prepared solutions of complexes **3** and **4**. After 3–4 weeks of aging, the TON is 20–30% lower than of freshly prepared solutions of **2**. Freshly prepared solutions of complex **3** are *ca.* 3 times less active and slower (TOF_{ap} ~0.025 s^{-1}) than freshly prepared solutions

of **2**. Complex **4** is inactive.[48] Therefore, the overall decrease of catalytic activity of stock solutions of **2** with aging may be caused by the transformation to **3** and **4**. The generation of $[Co(H_2O)_6]^{2+}$ during the decomposition in aged stock solutions is also likely to contribute to the final observed catalytic activity.

Hence, the intact **2** could well be a water oxidation catalyst. This is indicated by the following findings: (i) the oxidation of water in the presence of **2** proceeds much faster than in the presence of its decomposition products (**3** and **4**); (ii) the overall activity of stock solutions of **2** decreases very slowly with aging time; (iii) **2** is stable on the time-scale of the light-driven water oxidation process (~ 30 min).

Under turnover conditions the cobalt(s) centers in **2** are briefly in a higher oxidation state(s) than 2+. The oxidized form of **2** might both be less stable and decompose faster than **2** (all Co(II) centres) itself. We cannot assign the catalytic activity to a specific isomer (**2a** and **2b**).

Conclusions

We have synthesized and characterized a new tetracobalt-substituted polyoxometalate which co-crystallizes as a 1 : 1 mixture of two isomers. While thermodynamically unstable, this POM is likely to catalyze water oxidation in a light-driven system with $[Ru(bpy)_3]^{2+}$ and $S_2O_8^{2-}$ as the photosensitizer and sacrificial electron acceptor, respectively. Several decomposition products of **2** in solution were isolated and characterized. Their catalytic activity towards water oxidation is lower than for **2**.

Acknowledgements

The present research is supported by grant DE-FG02-03ER15461 from the U.S. Department of Energy. The authors gratefully acknowledge NSF MRI-R2 grant (CHE-0958205) and the use of the resources of the Cherry Emerson Center for Scientific Computation.

Notes and references

1 R. Eisenberg and H. B. Gray, *Inorg. Chem.*, 2008, **47**, 1697–1699.
2 Y. V. Geletii, Q. Yin, Y. Hou, Z. Huang, H. Ma, J. Song, C. Besson, Z. Luo, R. Cao, K. P. OHalloran, G. Zhu, C. Zhao, J. Vickers, Y. Ding, S. Mohebbi, A. E. Kuznetsov, D. G. Musaev, T. Lian and C. L. Hill, *Isr. J. Chem.*, 2011, **51**, 238–246.
3 S. W. Gersten, G. J. Samuels and T. J. Meyer, *J. Am. Chem. Soc.*, 1982, **104**, 4029–4030.
4 J. K. Hurst, J. Zhou and Y. Lei, *Inorg. Chem.*, 1992, **31**, 1010–1017.
5 T. Wada, K. Tsuge and K. Tanaka, *Angew. Chem. Int. Ed.*, 2000, **39**, 1479–1482.
6 M. Yagi and M. Kaneko, *Chem. Rev.*, 2001, **101**, 21–35.
7 J. K. Hurst, *Coord. Chem. Rev.*, 2005, **249**, 313–328.
8 R. Zong and R. Thummel, *J. Am. Chem. Soc.*, 2005, **127**, 12802–12803.
9 J. T. Muckerman, D. E. Polyansky, T. Wada, K. Tanaka and E. Fujita, *Inorg. Chem.*, 2008, **47**, 1787–1802.
10 J. J. Concepcion, J. W. Jurss, J. L. Templeton and T. J. Meyer, *J. Am. Chem. Soc.*, 2008, **130**, 16462–16463.
11 T. A. Betley, Y. Surendranath, M. V. Childress, G. E. Alliger, R. Fu, C. C. Cummins and D. G. Nocera, *Phil. Trans. R. Soc. B*, 2008, **363**, 1293–1303.
12 N. D. McDaniel, F. J. Coughlin, L. L. Tinker and S. Bernhard, *J. Am. Chem. Soc.*, 2008, **130**, 210–217.
13 R. Brimblecombe, G. F. Swiegers, G. C. Dismukes and L. Spiccia, *Angew. Chem. Int. Ed.*, 2008, **47**, 7335–7338.
14 X. Sala, I. Romero, M. Rodríguez, L. í. Escriche and A. Llobet, *Angew. Chem. Int. Ed.*, 2009, **48**, 2842–2852.
15 J. F. Hull, D. Balcells, J. D. Blakemore, C. D. Incarvito, O. Eisenstein, G. W. Brudvig and R. H. Crabtree, *J. Am. Chem. Soc.*, 2009, **131**, 8730–8731.
16 J. J. Concepcion, J. W. Jurss, M. K. Brennaman, P. G. Hoertz, A. O. T. Patrocinio, N. Y. M. Iha, J. L. Templeton and T. J. Meyer, *Acc. Chem. Res.*, 2009, **42**, 1954–1965.
17 S. Masaoka and K. Sakai, *Chem. Lett.*, 2009, **38**, 182–183.
18 L. Duan, Y. Xu, M. Gorlov, L. Tong, S. Andersson and L. Sun, *Chem. Eur. J.*, 2010, **16**, 4659–4668.
19 W. C. Ellis, N. D. McDaniel, S. Bernhard and T. J. Collins, *J. Am. Chem. Soc*, 2010, **132**, 10990–10991.
20 V. Y. Shafirovich and A. E. Shilov, *Kinet. Katal.*, 1979, **20**, 1156–1162.
21 V. Y. Shafirovich, N. K. Khannanov and V. V. Strelets, *Nouveau J. Chim.*, 1980, **4**, 81–84.
22 A. Harriman, I. J. Pickering, J. M. Thomas and P. A. Christensen, *J. Chem. Soc. Faraday Trans. 1*, 1988, **84**, 2795–2806.
23 D. M. Robinson, Y. B. Go, M. Greenblatt and G. C. Dismukes, *J. Am. Chem. Soc*, 2010, **132**, 11467–11469.
24 Y. Gorlin and T. F. Jaramillo, *J. Am. Chem. Soc.*, 2010, **132**, 13612–13614.
25 N. D. Morris, M. Suzuki and T. E. Mallouk, *J. Phys. Chem. A*, 2004, **108**, 9115–9119.
26 W. J. Youngblood, S.-H. A. Lee, Y. Kobayashi, E. A. Hernandez-Pagan, P. G. Hoertz, T. A. Moore, A. L. Moore, D. Gust and T. E. Mallouk, *J. Am. Chem. Soc.*, 2009, **131**, 926–927.
27 H. Han and H. Frei, *J. Phys. Chem. C*, 2008, **112**, 16156–16159.
28 M. W. Kanan and D. G. Nocera, *Science*, 2008, **321**, 1072–1075.
29 M. W. Kanan, Y. Surendranath and D. G. Nocera, *Chem. Soc. Rev.*, 2009, **38**, 109–114.
30 F. Jiao and H. Frei, *Angew. Chem. Int. Ed.*, 2009, **48**, 1841.
31 M. T. Pope and A. Müller, *Angew. Chem.*, 1991, **103**, 56–70.
32 C. L. Hill and C. M. Prosser-McCartha, *Coord. Chem. Rev.*, 1995, **143**, 407–455.
33 C. L. Hill, *Chem. Rev.*, 1998, **98**, 1–2.
34 M. T. Pope, and A. Müller, ed., *Polyoxometalate Chemistry From Topology* via *Self-Assembly to Applications*, Kluwer Academic Publishers, Dordrecht, 2001.
35 J. J. Borrás-Almenar, E. Coronado, A. Müller, and M. T. Pope, *Polyoxometalate Molecular Science*, Kluwer Academic Publishers, Dordrecht, 2003.
36 U. Kortz and A. Müller, *J. Cluster Sci.*, 2006, **17**, 139–141.
37 C. L. Hill, in *Comprehensive Coordination Chemistry-II: From Biology to Nanotechnology*, ed. A. G. Wedd, Elsevier Ltd, Oxford, UK, 2004, vol. 4, pp. 679–759.
38 D.-L. Long, E. Burkholder and L. Cronin, *Chem. Soc. Rev.*, 2007, **36**, 105–121.
39 Y. V. Geletii, B. Botar, P. Kögerler, D. A. Hillesheim, D. G. Musaev and C. L. Hill, *Angew. Chem. Int. Ed.*, 2008, **47**, 3896–3899.
40 A. E. Kuznetsov, Y. V. Geletii, C. L. Hill, K. Morokuma and D. G. Musaev, *J. Am. Chem. Soc.*, 2009, **131**, 6844–6854.
41 Y. V. Geletii, Z. Huang, Y. Hou, D. G. Musaev, T. Lian and C. L. Hill, *J. Am. Chem. Soc.*, 2009, **131**, 7522–7523.
42 Y. V. Geletii, C. Besson, Y. Hou, Q. Yin, D. G. Musaev, D. Quinonero, R. Cao, K. I. Hardcastle, A. Proust, P. Kögerler and C. L. Hill, *J. Am. Chem. Soc.*, 2009, **131**, 17360–17370.
43 A. Sartorel, M. Carraro, G. Scorrano, R. D. Zorzi, S. Geremia, N. D. McDaniel, S. Bernhard and M. Bonchio, *J. Am. Chem. Soc*, 2008, **130**, 5006–5007.
44 A. Sartorel, P. Miro, E. Salvadori, S. Romain, M. Carraro, G. Scorrano, M. D. Valentin, A. Llobet, C. Bo and M. Bonchio, *J. Am. Chem. Soc.*, 2009, **131**, 16051–16053.
45 M. Orlandi, R. Argazzi, A. Sartorel, M. Carraro, G. Scorrano, M. Bonchio and F. Scandola, *Chem. Commun.*, 2010, **46**, 3152–3154.
46 F. Puntoriero, G. L. Ganga, A. Sartorel, M. Carraro, G. Scorrano, M. Bonchio and S. Campagna, *Chem. Commun.*, 2010, **46**, 4725–4227.
47 C. Besson, Z. Huang, Y. V. Geletii, S. Lense, K. I. Hardcastle, D. G. Musaev, T. Lian, A. Proust and C. L. Hill, *Chem. Commun.*, 2010, 2784–2786.
48 Q. Yin, J. M. Tan, C. Besson, Y. V. Geletii, D. G. Musaev, A. E. Kuznetsov, Z. Luo, K. I. Hardcastle and C. L. Hill, *Science*, 2010, **328**, 342–345.
49 L.-Z. Zhang, W. Gu, X. Liu, Z. Dong, Y.-S. Yang, B. Li and D.-Z. Liao, *Inorg. Chem. Comm.*, 2007, **10**, 1378–1380.

50 A. Tézé and G. Hervé, in *Inorg. Synth.*, ed. A. P. Ginsberg, John Wiley and Sons, New York, 1990, vol. 27, pp. 85–96.
51 Y.-Z. Zheng, M. Speldrich, H. Schilder, X.-M. Chen and P. Kögerler, *Dalton Trans.*, 2010, **39**, 10827–10829.
52 I. L. Malaestean, M. Speldrich, S. G. Baca, A. Ellern, H. Schilder and P. Kögerler, *Eur. J. Inorg. Chem.*, 2009, 1011–1018.
53 I. Bruker AXS, *Analytical X-ray Systems*, Madison, WI, 2003.
54 I. Bruker AXS, *Analytical X-Ray Systems*, Madison, WI, 2003.
55 G. Sheldrick, 2.10 edition edn, 2003.
56 I. Bruker AXS, Madison, WI, 2003.
57 M. Speldrich, H. Schilder, H. Lueken and P. Kögerler, *Isr. J. Chem.*, 2011, **51**, 215–227.
58 Z. Huang, Z. Luo, Y. V. Geletii, J. Vickers, Q. Yin, D. Wu, Y. Hou, Y. Ding, J. Song, D. G. Musaev, C. L. Hill and T. Lian, *J. Am. Chem. Soc.*, 2011, **133**, 2068–2071.
59 A. L. Kaledin, Z. Huang, Y. V. Geletii, T. Lian, C. L. Hill and D. G. Musaev, *J. Phys. Chem. A*, 2010, **114**, 73–80.
60 A. L. Kaledin, Z. Huang, Q. Yin, E. L. Dunphy, E. C. Constable, C. E. Housecroft, Y. V. Geletii, T. Lian, C. L. Hill and D. G. Musaev, *J. Phys. Chem. A*, 2010, **114**, 6284–6297.
61 T. J. R. Weakley and S. A. Malik, *J. Inorg. Nucl. Chem.*, 1967, **29**, 2935–2944.
62 N. Laronze, J. Marrot and G. Herve, *Chem. Commun.*, 2003, 2360–2361.
63 N. Leclerc-Laronze, J. Marrot and G. Herve, *Inorg. Chem.*, 2005, **44**, 1275–1281.
64 J. H. Coates, G. J. Gentle and S. F. Lincoln, *Nature*, 1974, **249**, 773–775.
65 J. Baes, F. Charles and R. E. Mesmer, *The Hydrolysis of Cations*, John Wiley & Sons, New York, 1976.